Velocity of movement of actin filaments in in vitro motility assay

Measured by fluorescence correlation spectroscopy

J. Borejdo and S. Burlacu
Baylor Research Institute, Baylor University Medical Center, Dallas, Texas 75226

ABSTRACT We have measured the velocity of actin filaments in in vitro motility assay by fluorescence correlation spectroscopy. In this method, one measures fluctuations in the number of filaments in an open sample volume. The number of filaments was calculated from measurements of fluorescence of rhodamine-phalloidin bound to F-actin. Sample volume was defined by a diaphragm placed in front of the photomultiplier. Fluctuations arise when actin filaments enter and leave the sample volume due to translations driven by mechanochemical interactions with myosin heads which are immobilized on a glass surface. The average velocity of the translation of filaments determined by the correlation method, $\langle V_c \rangle$, was equal to the diameter of the diaphragm devided by the half-time of the relaxation of fluctuations. The average number of moving filaments determined by correlation method, $\langle N_c \rangle$, was inversely proportional to the relative fluctuations. By the fluctuation method it was possible to determine the average velocity of over 800 moving filaments in <4 min. There was good agreement between $\langle V_c \rangle$ and $\langle N_c \rangle$ and the average velocity and the average number of moving filaments determined manually. To be able to apply correlation measurements to an experimental problem, neither $\langle V_c \rangle$ nor $\langle N_c \rangle$ must depend on the position of observation of filaments. We first confirmed that this was indeed the case. We then applied the method to investigate the dependence of motility on the ATPase activity of myosin heads. ATPase activity was varied by mixing intact heads with heads which were labeled with different thiol reagents. It was found that the motion was drastically influenced by the reagent used for modification. When the reagent was *N*-ethyl-maleimide, 1.5% modification was sufficient to completely inhibit the motion. When the reagent was 5-iodoacetamidofluorescein, motion declined hyperbolically with the fraction of modified heads.

INTRODUCTION

In an in vitro motility assay one observes in the light microscope the motion of individual actin filaments being propelled by the myosin heads which are immobilized on a glass surface (Kron and Spudich, 1986; Harada and Yanagida, 1988; Toyoshima et al., 1990; Uyeda et al., 1990; Harada et al., 1990). Motion is analyzed to yield the mean velocity of actin filaments, which when combined with the rate of hydrolysis of ATP, leads to important implications about the mechanism of muscle contraction (for review see Huxley, 1990). Velocity can be measured manually (by overlaying a plastic sheet on a video monitor or by using a cursor superimposed on the video image, Kron et al., 1991), by automatic tracking) when actin filaments are all parallel, Sheetz et al., 1986) and probably by using a dedicated video-based system (quoted in Kron et al., 1991). In vitro work shows that there remains a need for a precise and rapid method to measure velocity and the number of moving actin filaments, a method which would be independent of the observer's objectivity and be free from lag and image distortion associated with video imaging of faint objects. Here we present a method of measuring velocity and the number of filaments which does not require imaging of filaments: we analyze the fluctuations in light intensity arising from the change in the number of the actin filaments present in the sample volume. The number of filaments is determined by fluorescence. The sample volume is defined by a diaphragm placed in front of the photomultiplier. The mean number of filaments in the sample volume is constant, but at any instant the actual number fluctuates as filaments enter and leave the volume due to the translations associated with the splitting of ATP. The translations give rise to fluctuations in the photocurrent, which are analyzed to yield the autocorrelation function (ACF). The decay of the ACF measures the relaxation of fluctuations to the mean value of the photocurrent. When the velocity of translation was defined as a ratio of the diameter of the diaphragm to the half time of relaxation, the method gave good agreement with velocities of the same filaments measured manually. The mean number of moving filaments determined by the correlation method also gave good agreement with the numbers measured manually. We first used the correla-

Abbreviations used in this paper: TRITC-phalloidin: tetramethylrhodamine-isothiocyanate-phalloidin; 5-IAF: 5-iodoacetamidofluorescein; NEM: *N*-ethyl-maleimide; HMM: heavy meromyosin; FFT: fast Fourier transform; ACF: Autocorrelation function; rms: root mean square; SD: standard deviation; SE: standard error.

tion method to check that the average velocity and the number of moving filaments was independent of the position of observation relative to the point of application of ATP. We then varied ATPase activity of HMM by chemical modification with two different thiol reagents. We found that when the reagent was *N*-ethylmaleimide, small modification was sufficient to completely inhibit the motion and that when the reagent was 5-iodoacetamidofluorescein, motion declined hyperbolically with the fraction of modified heads.

GENERAL PRINCIPLES

Optics and electronics

The microscope system used to measure the fluctuations in fluorescence intensity caused by the translating actin filaments is shown in Fig. 1. An Argon ion laser (Spectra Physics Model 164-03, Mountain View, CA) generates a vertically polarized beam of 514.5 nm light, which has a Gaussian intensity profile. The stabilization accessory (Liconix Model 50SA, Sunnyvale, CA) reduces the noise in the light output to less than 0.01% rms. The beam is attenuated by the neutral density filters (ND). Typically, 1.5 mW is incident on the auxiliary lens (AL). AL adjusts the focus of the beam that it does not coincide with the front focal plane of the objective. As a result the filaments in the object plane are not illuminated with a sharply focused beam of light, but instead are illuminated with a disk of light with an "effective" radius of ~15 μm. The laser power incident on the sample is typically 0.15 mW. A dichroid mirror (DM) directs all wavelengths below 580 nm at the sample (S) placed on a stage of a Zeiss Standard microscope. The fluorescent light is collected through X100 Neofluar (N.A. = 1.3) objective, passed through a barrier filter into a circular field diaphragm (FD) with a diameter D. The role of a diaphragm is to precisely define the field of view of the photomultiplier (PM): the circular diaphragm used in these experiments had a diameter in the sample plane of either 5 or 10 μm. Field of view is monitored by the SIT camera (Cohu Model 5000, San Diego, CA) and the video signal is recorded on a VCR (Sharp VC6610U, Mahwah, NJ). The camera is attached in parallel with the PM through a specially constructed beam splitter (CRG Electronics, Houston, TX). The light is photon counted by the PM, amplified (Pacific Instruments Video Amplifier, Concord, CA), discriminated (LeCroy Model 620 CL, Spring Valley, NY) and fed to a home built inverter which converts the negative going NIM output of the discriminator to a standard TTL signal suitable for counting by a 16 bit latch counter (MetraByte Model CTM-05, Taunton, MA) installed in an IBM PC. A series of 16 bit integer numbers representing PM counts which have accumulated in a "bin width" are stored on a disk for subsequent analysis (see below).

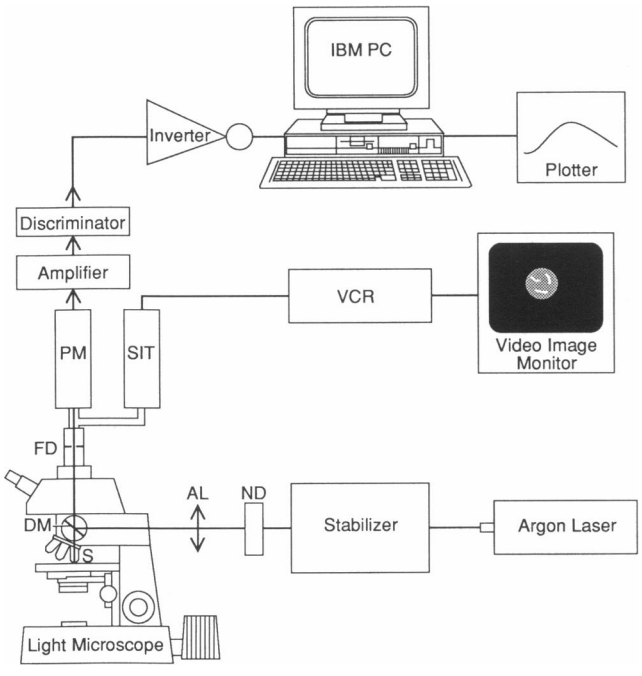

FIGURE 1 Fluorescence correlation spectrometer to measure the velocity of translation of actin filaments. *ND:* neutral density filters; *AL:* auxiliary lens; *FD:* field diaphragm; *PM:* photomultiplier; *SIT:* silicon intensified target video camera.

Data analysis

Groups of 1,024 numbers (sweeps) are analyzed separately. Data in each sweep is fitted by the least squares to a straight line. Every point on a line is subtracted from the corresponding data point to correct for the slow drift in fluorescence intensity due to the photobleaching. The first and last 64 data points of the resulting sequence of 1,024 points are smoothed to prevent aliasing and prepared for Fourier transformation as previously described (Borejdo and Morales, 1977). Fast Fourier transform (FFT) (Rabiner and Gold, 1975) is applied to each sequence of 1,024 points to give the power spectrum of the signal, and the procedure is repeated on subsequent sequences (if any). The power spectra are averaged and inverse Fourier Transformed to give the ACF.

Random errors

A measure of random errors is signal-to-noise ratio (S/N). In number fluctuation experiments S/N depends on σ, the rate of detection of the fluorescent photons per molecule of the dye during time interval $\delta\tau$ (bin width) (Magde et al., 1974). In our experiments it is

$$\sigma = g\epsilon QP\delta\tau/\pi\omega^2, \quad (1)$$

where g is the efficiency with which the photomultiplier sees the emitted photons, ϵ is the extinction coefficient of fluorophore, Q is its quantum yield, P is the laser light intensity, ω is the effective radius of the laser beam, and $\delta\tau$ is the bin width. In a typical experiment, $g = 1.5 \times 10^{-4}$ (geometrical collection efficiency of the objective is 2.5×10^{-2} while the field diaphragm allows only $1/150$ of the light to pass to the PM), $\epsilon = 3 \times 10^4$ $M^{-1}cm^{-1} = 1.5 \times 10^{-16}$ cm^2 per rhodamine molecule, $Q = 1$ (Borejdo et al., 1979 and because quantum yield of rhodamine-phalloidin increases when it binds to actin; Yanagida et al., 1985), $\delta\tau$ is 100 ms, P is 0.15 mW ($P = 3.9 \times 10^{14}$ green photons/sec), and $\omega = 5$ μm. Eq. 1 gives $\sigma = 1.1$ This is a high number, and is obtainable only because we are observing slow motions of highly fluorescent molecules through an objective with high N.A. It can be shown that when σ is greater or equal to 1, then

$$S/N = (M\delta\tau/2\tau_D)^{1/2}, \quad (2)$$

(Koppel, 1974; Magde et al., 1974) where M is the total number of bins collected, $\delta\tau$ is the bin width and τ_D is the characteristic time of the

ACF. In other words, when the rate of detection is high, the S/N ratio does not depend on the light flux. Rather, it is equal to the square root of the half of the ratio of the length of the observation time to the characteristic time of the fluctuations. In a typical experiment, M = 2048, $\delta\tau$ = 100 ms and τ_D = 1 s giving S/N = 10.

Systematic errors

Magde et al. (1974) classified these errors as arising from electronics, optics and the solution itself. We did not detect any spurious fluctuations arising from the first two (see Fig. 5 *B* below). The most obvious source of the fluctuations which arise from the solution itself was photobleaching. In spite of the fact that our solution contained a deoxygenating system (Englander et al., 1987) and that the light flux was low (intensity was typically 0.15 mW) we observed some photodegradation (Fig. 5 *A*). However, the quantum yield for photobleaching, which was measured by following the decrease in emitted light intensity of actin filaments in rigor, was extremely low. In the experiment illustrated in Fig. 5 it was smaller than 10^{-11}. Lifetime for bleaching was about 500 s, much longer than the characteristic time for the translation of actin filaments (see below).

METHODS

Materials

Tetramethyl-rhodamine-isothiocyanate-phalloidin (TRITC-phalloidin), *N*-ethyl-maleimide (NEM), bovine serum albumin (BSA) and ATP were from Sigma Chemical Co. (St. Louis, MO). β-mercaptho-ethanol was from BioRad (Richmond, CA). 5-iodo-acetamido-fluorescein (5-IAF) was from Molecular Probes (Eugene, OR). Fluorescent microspheres (Fluoresbrite Plain Microspheres) were from Polysciences (Warrington, PA) and nitrocellulose was from Fullham (Latham, NY).

Solutions

TRITC-phalloidin was prepared as follows: 0.1 mg was dissolved in 0.1 mL of 50% methanol and diluted 10 times with 25 mM K-Acetate, 25 mM TRIS-Acetate pH 7.5. Motility was measured in an A-buffer containing 25 mM KAcetate, 25 mM TRIS-Acetate buffer pH 7.5, 4 mM Mg_2SO_4, 1% β mercapthoethanol and 1 mM EGTA.

Protein preparation and labeling

Actin and HMM were prepared according to Spudich and Watt (1971) and Weeds and Pope (1977), respectively. F-actin was labeled with TRITC-phalloidin by adding 0.05 mg/mL protein to an equimolar concentration of the dye followed by an overnight incubation on ice. After staining F-actin it was diluted with A-buffer to 10 nM. HMM was modified with 5-IAF or NEM by a 45 min incubation with 10× molar excess of the dye on ice. The reaction was stopped by adding a large excess of β-mercapthoethanol and HMM was dialyzed overnight against the A-buffer. Nearly every myosin head carried 1 molecule of 5-IAF or NEM. Modified HMM had no EDTA ATPase activity.

Motility assay

The movement of phalloidin labeled actin was induced similarly as described by Kron and Spudich (1986). Briefly: flow cells were constructed from a glass slide separated from the coverslip by a coverslip glued to the slide by superglue (PC Zip, Adhesive Solutions, Sydney, Australia). The sample volume was ~100 μL. The inner surface of the coverslip was precoated with nitrocellulose. HMM (25–600 μg/mL) was introduced to the flow cell for a few minutes and washed with the A-buffer. Except in the experiments in which HMM was modified with NEM, heads which were unable to dissociate from actin in the presence of ATP were blocked by washing with the A-buffer containing unlabeled F-actin and 2 mM ATP. 10 nM of rhodamine phalloidin labeled F-actin was introduced to a flow cell, incubated for several minutes with immobilized HMM and the excess was washed out with the A-buffer. To initiate the motion of filaments, 2 mM ATP in A-buffer which contained the oxygen scavenging system (Englander et al., 1987), was introduced to the flow cell by applying it to one side of the cell and sucking it with the blotting paper on the other side.

Measurements of the lengths of actin filaments

The spatial resolution of an optical microscope is determined by the diffraction limit of the objective lens. In our case, this limit corresponds to a pixel size in the image of ≈0.19 μm. In practice, the images on the video monitor were magnified 2,750 times and any luminous object that was shorter than ≈1.1 mm on the monitor screen was included in the population having length less than 0.5 μm. The width of a single filament is smaller than the resolution of the optical microscope. The fact that it was visible at all was due to the "magnification anisotropy" (Houseal et al., 1989), i.e., the fact that its width was magnified ~3,500 times, while its length was magnified by the magnification of the microscope, i.e., 125 times.

Individual frames were grabbed from the VCR by a MVI frame grabber (MetraByte Corp, Tauton, MA) which was operated by an AT type computer. The images were contrast enhanced by stretching the gray levels to a full range between 0 (black) and 255 (white) using a video analysis program (Java 1.4, Jandel Scientific, Corte Madera, CA), equalized using Gray F/X gray scale editor (Xerox Imaging Systems, Sunnyvale, CA) and printed on Video Printer (Sony, Teaneck, New Jersey). The contour length of filaments was measured by the "distance" function of Java image analysis program. The histograms were obtained by counting "by range" filaments of a given length. They were plotted using SigmaPlot 4.1 (Jandel Scientific, Corte Madera, CA).

RESULTS

Diffusion

In a confocal microscope system such as used here, the decay time of the ACF depends on the relative size of the diaphragm and the diameter of the laser beam (Qian and Elson, 1991). Detailed analysis of the optics of the measurement system is therefore required to obtain exact expression for the ACF. Nevertheless, it is possible to avoid solving this difficult problem by carrying out empirical calibrations using particles with well characterized diffusion coefficients. Below, we carry out such calibrations to show that in our system, even in the case of three-dimensional diffusion of large (but monodisperse) particles, the two-dimensional analysis of Elson and Magde (1974) is valid. We measured the ACF of the monodisperse suspension of particles of size similar to

actin filaments. We used fluorescent polystyrene latex microspheres 1 ± 0.05 μm in diameter diluted with water to ~5–50 × 10^6 particles/mm^3. Fig. 2 shows the appearance of the spheres through the field diaphragm with D = 10 μm (the image is of poor quality because the spheres execute rapid Brownian motion which makes it difficult to record spheres on a VCR and to grab images by a frame grabber). This sample gave a mean rate of photon arrival of $\langle n \rangle$ = 3,948 photons/bin width. The observed rms fluctuation was 772 counts/s (i.e., the relative rms fluctuation, β, was 19.5%). The theoretical fluctuation for white noise signal is 62.8 counts/s ($=\langle n \rangle^{1/2}$, Rabiner and Gold, 1975). In this experiment the observed fluctuation was 12 times greater than the fluctuation expected from the white noise signal. β was so large because the number of fluorescent objects in the field of view is small (see below). These values were typical of all sphere experiments.

The ACF of a photocurrent signal of preparation shown in Fig. 2 is shown in Fig. 3. Elson and Magde (1974) showed that the photocurrent autocorrelation function, $G(\tau)$, for two-dimensional diffusion of single fluoresecent species was:

$$G(\tau) = (g\epsilon Q)^2 P^2 LC(\pi\omega^2)^{-1}[1 + \tau/\tau_D]^{-1} \qquad (3)$$

where g, ϵ, Q, P and ω are as before. L is the optical path length (in this experiment equal to the depth of focus of the objective, 1.3 μm) and C is the mean concentration of the solute. The characteristic time for diffusion is $\tau_D = \omega^2/4D_D$ where D_D is the diffusion coefficient for solute D. A spike at $\tau = 0$ due to the shot noise of the photomultiplier is not included in Eq. 3. Eq. 3 (Fig. 3, *dotted line*) fits the experimental data well (for example, a single exponential function would not fit) in spite of the fact that our experimental arrangement differed from that for which Eq. 3 was derived. The characteristc time of the ACF was 2.32 s giving $D_D = \omega^2/4\tau_D = 0.67 \times 10^{-8}$ cm^2s^{-1} (ω = 2.5 μm). The theoretical value for the diffusion coefficient of spheres 1 μm in diameter at room temperature is 0.42 × 10^{-8} cm^2s^{-1} (Tanford, 1963) in good agreement with our observations. Thus, two-dimensional analysis of the diffusion (as expressed by Eq. 3) is, in our microscope system with $\omega = D/2$, a good approximation of a diffusion in three dimensions.

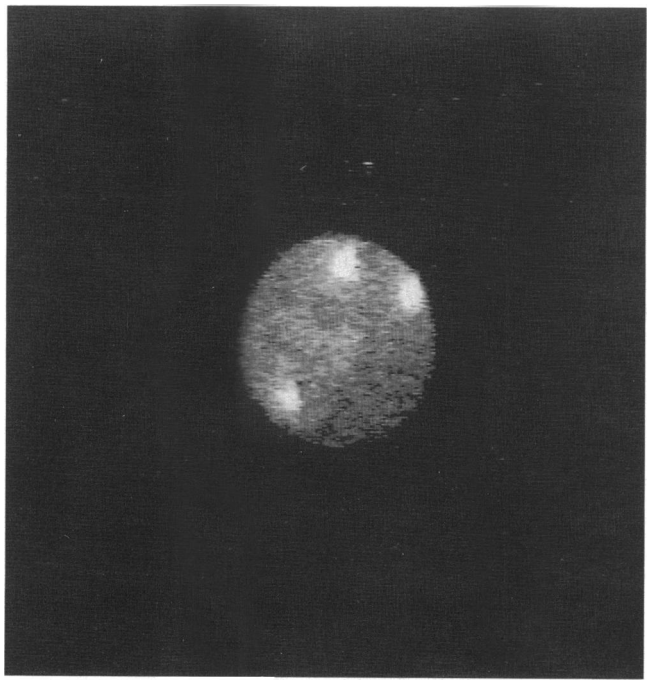

FIGURE 2 Fluorescent microspheres 1 μm in diameter as seen through a diaphragm 10 μm in diameter.

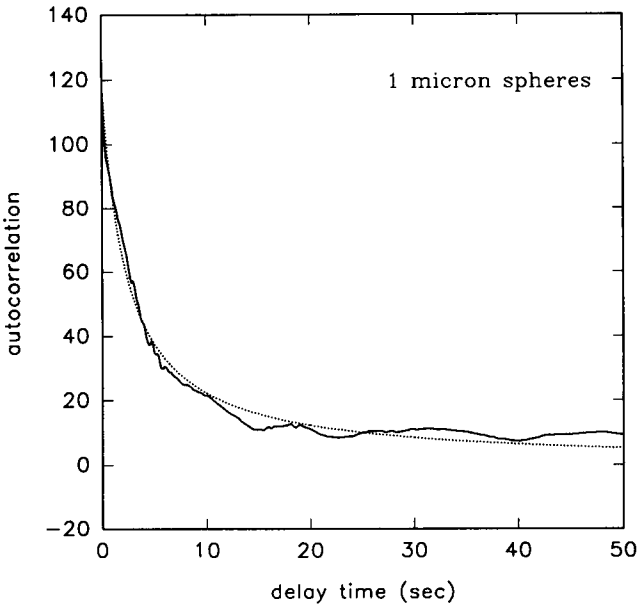

FIGURE 3 The correlation function (*solid line*) for fluorescent microspheres of 1 ± 0.05-μm diameter diffusing freely through an aqueous solution and detected through a 5-μm diameter field diaphragm. (*Dotted line*) fit to Eq. 3. The data were collected for 204.8 s.

Stationary actin filaments

The appearance of stationary actin filaments as seen by the photomultiplier is shown in Fig. 4*A*. The light intensity is the highest at the center of the field and decreases towards the edges. This is a result of the Gaussian character of the intensity profile of the laser beam. The central portion of the field is selected by a field diaphragm (Fig. 4*B*). When actin filaments are stationary (in rigor solution), the intensity of the light

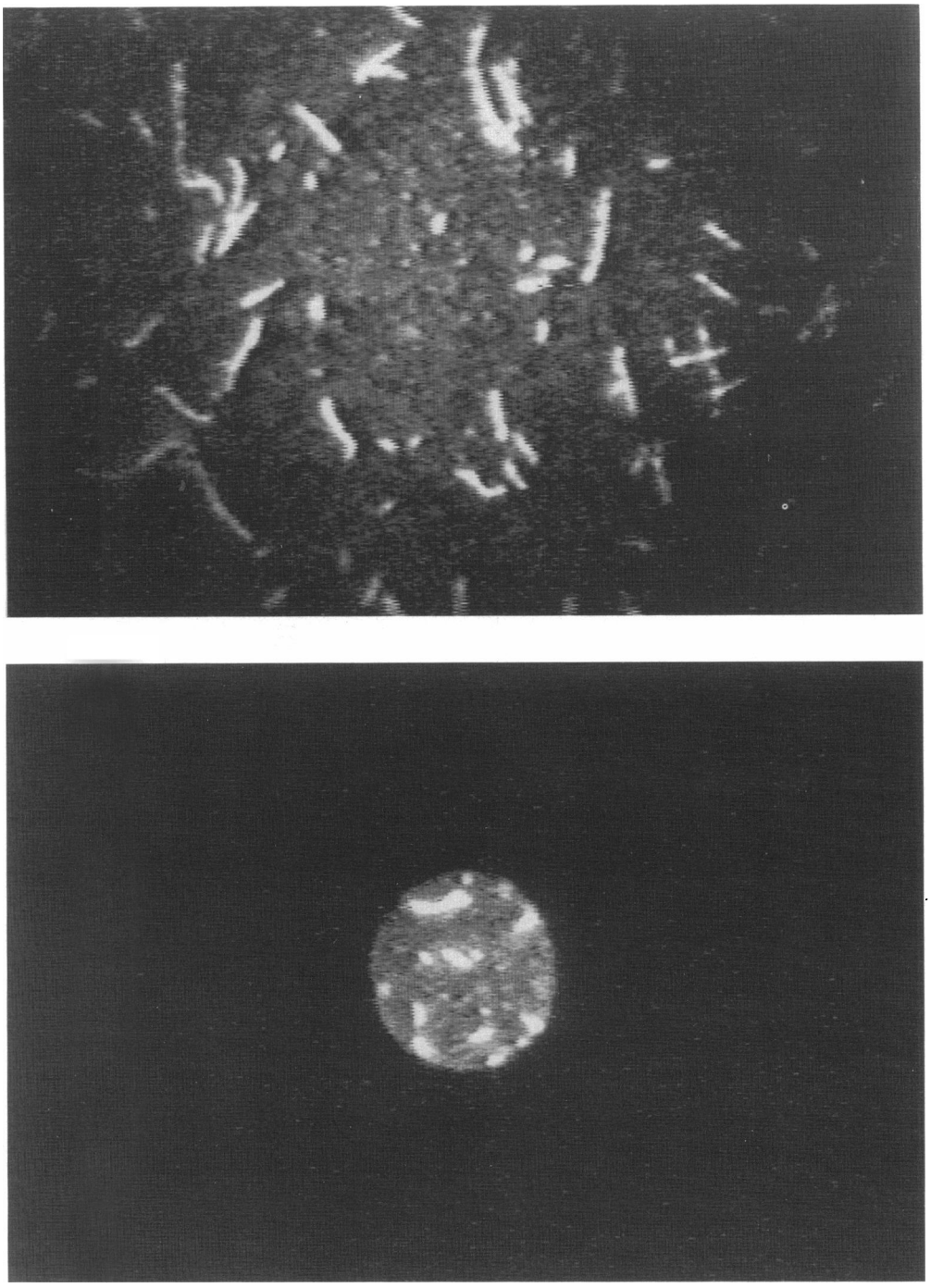

FIGURE 4 (*A*) Actin filaments in A-buffer (rigor). (*B*) same filaments 9 min after adding 2 mM ATP and deoxygenating system to filaments in rigor. Diameter of the diaphragm was 10 μm.

impinging on the photocathode of the photomultiplier is constant. The signal is shown in Fig. 5 *A*. The mean rate of photon arrival was $\langle n \rangle$ = 1060/bin width. The observed rms fluctuation was 34.5 counts/s (β = 3.2%). The theoretical fluctuation for white noise signal was 32.5 counts/s. In this experiment the observed fluctuation was therefore pratically equal to fluctuation expected from the white noise signal.

The ACF of stationary filaments is shown in Fig. 5 *B*. The fact that the autocorrelation function is flat proves

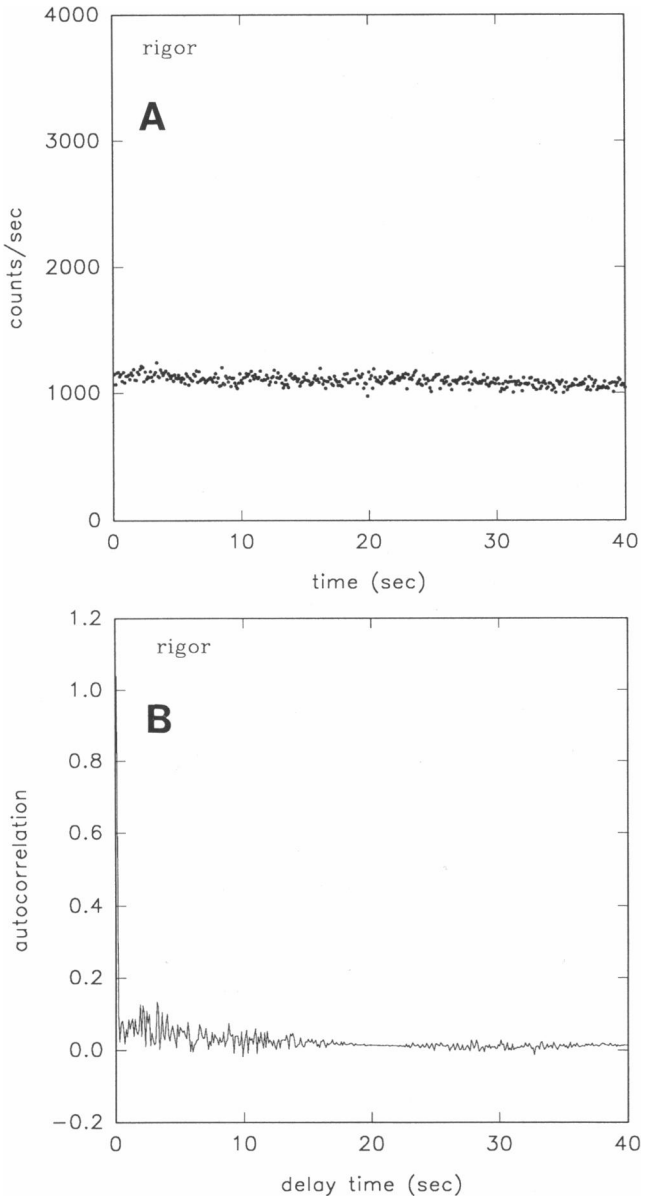

FIGURE 5 (*A*) photocurrent signal of filaments in rigor as seen through diaphragm 5 μm in diameter. (*B*) autocorrelation function of signal shown in *A*.

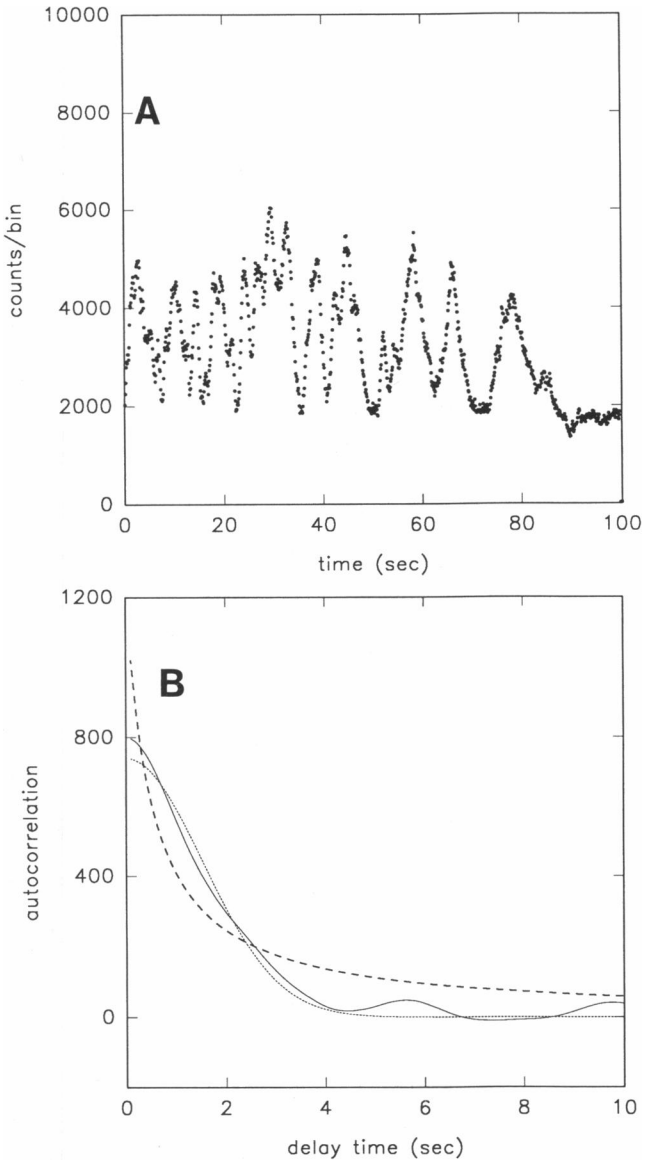

FIGURE 6 (*A*) photocurrent signal obtained during translation of filaments through diaphragm 5 μm in diameter. (*B*) (*solid line*) autocorrelation function of signal shown in (A) (*dotted line*) fit to Eq. 4; (*broken line*) fit to Eq. 3.

that the detection optics and electronics are free of spurious correlations.

Mobile actin filaments

Fig. 6 *A* shows the photocurrent signal of the filaments moving in the presence of 2 mM ATP. Fluctuations in the photocurrent arise because actin filaments, propelled by interaction with HMM, move in and out of the field of view defined by the diaphragm. $\langle n \rangle$ was 3,198 counts/bin. The observed rms fluctuation was 1,089 counts/s (relative fluctuation $\beta = 34\%$). If the signal had white noise characteristics the theoretical fluctuation would have been $(3{,}198)^{1/2} = 56$ counts/s (1.7%). These values were typical of all in vitro experiments.

The ACF is shown as a solid line in Fig. 6 *B*. Magde and Elson (1978) derived the following expression for the autocorrelation function of uniformly translating

particles

$$G(\tau) = (g\epsilon Q)^2 P^2 LC(\pi\omega^2)^{-1} \exp[-(V\tau/\omega)^2], \quad (4)$$

where all the symbols have the same meaning as in Eq. 3 and V is the velocity of translation. The dotted line in Fig. 6 *B* is the fit to Eq. 4 with $V = 1.18$ μm/s ($\omega = 2.5$ μm). Eq. 3 (*broken line*), or a single exponential (not shown) gave a poor fit.

In the majority of experiments, however, the ACF could not be fitted to Eq. 4 (likely due to the variability in size distribution of actin filaments, see Discussion). More typical ACF's are shown in Fig. 7. Sometimes correlation functions declined rapidly and then oscillated with a characteristic frequency of about 0.4 Hz (as in Fig. 7 *A*). In other cases, the correlation functions declined linearly with delay time (as in Fig. 7 *B*). In either case a fit to Eq. 4 (*broken lines*) was poor. A much better fit could be achieved by, for example, a straight line in a region where ACF decayed rapidly with time, and another straight line in a region where ACF relaxed slowly to 0. As a figure of merit for the fit we used the normalized residual $N{:}N$ = square root of the sum of squares of residuals of the Marquardt-Levenberg fit. Experiments which gave poor fit to Eq. 4 were designated as those in which $N/G(0) > 1$; they constituted more than half of all experiments (13/23). To extract the velocity from all experiments, we defined the characteristic time $\tau_{1/2}$ as time required for ACF to decay to ½ of its value at $\tau = 0$. The average velocity of the filaments, $\langle V_c \rangle$, was defined as the ratio of the diameter of the diaphragm D to the characteristic time $\tau_{1/2}$, $\langle V_c \rangle = D/\tau_{1/2}$.

Comparison of velocities determined by correlation and manual methods

We compared the velocity determined by the correlation method (with characteristic time = $\tau_{1/2}$) with the mean velocity of the same filaments measured mannually ($\langle V_m \rangle$). To be sure that we followed the motion of the same filaments which contributed to the ACF, we recorded the motion of the filaments on VCR tape immediately after recording the autocorrelation signal. Velocity was measured manually as follows: a transparency film was laid over the video screen and the beginning of a filament at time 0 was marked by a pen. The VCR tape was advanced by 1 frame (1/30 s) and a new position was marked. The velocity was equal to the distance translated in 30 frames. $\langle V_m \rangle$ was an average velocity of 65 filaments in 23 different fields of view. $\langle V_m \rangle$ was 4.6 ± 0.6 μm/s (mean ± SD, min = 3.4 μm/s, max = 6.0 μm/s). The mean "pathlength" (distance between the visible changes of direction of actin) was

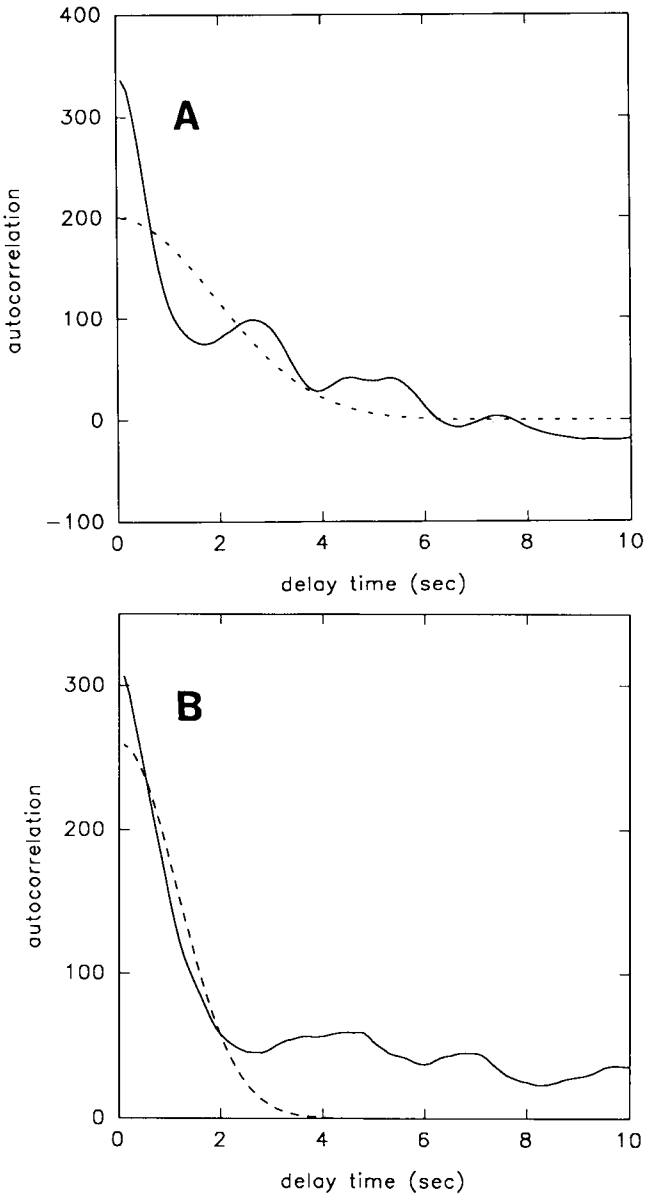

FIGURE 7 Examples of autocorrelation functions of translating filaments which could not be fitted to Eq. 4.

6.0 ± 2.9 μm (mean ± SD of 42 measurements in 23 different fields of view, min = 2.2 μm, max = 12 μm). The velocity determined by the correlation method $\langle V_c \rangle$ was 5.2 ± 2.0 μm/s (mean ± SD of 23 experiments, min = 2.3 μm/s, max = 8.8 μm/s). In Fig. 8 the $\langle V_m \rangle$ is plotted along the X-axis and $\langle V_c \rangle$ is plotted along the Y-axis. Solid horizontal and vertical lines are drawn through the means of velocities. The agreement between the two was good: according to the paired t-test the means were not different at 5% level of significance ($t = -1.34, P = 0.19$).

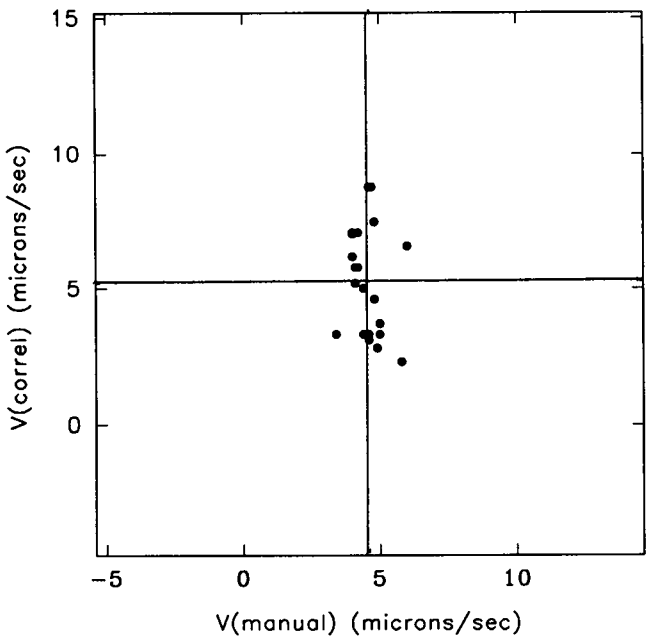

FIGURE 8 Average velocity of filaments determined by correlation method vs velocity determined manually. The solid lines indicate means of velocities.

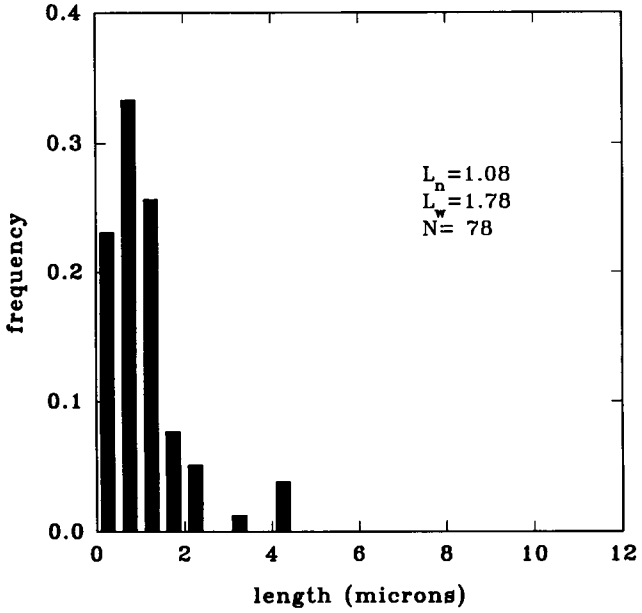

FIGURE 9 The distribution of lengths of actin filaments ~9 min after adding ATP. Histograms shows the number average length of filaments (L_n), weight average length of filaments (L_w), and number of filaments analyzed (N).

Correction for filament lengths

Eqs. 3 and 4 were derived for infinitesimally small molecules. In our experiments, however, the length of actin filaments constitutes a non-negligible fraction of the diameter of the diaphragm. This introduces two types of error. The first is that longer filaments remain in the area defined by the diaphragm for a longer period of time than the short ones. The second is that the long filaments contribute disproportionately more to the correlation function. The effect is that the correlation method underestimates velocity. A calculation shows (see Discussion) that the underestimation due to the first type of error is of the order of $\phi = L_n/D$ where L_n is the average length of actin filaments and D is the diameter of the diaphragm. Below, we measure L_n during the time when the correlation data was collected. Correlation and video data was collected as described above, i.e., care was taken to make sure that the same filaments which contributed to ACF were recorded. Histograms were calculated as described in Methods. Fig. 9 shows the distribution of filament sizes during data collection. The number average length of the filaments was defined as $L_n = (\Sigma N_i X_i)/(\Sigma N_i)$ where X_i is the length assigned to every filament whose length L_i was larger or equal to $X_i - 0.25$ μm and smaller than $X_i + 0.25$ μm (i.e., all filaments which differed in length by less than 0.5 μm were assigned the same length). The weight average length was defined as $L_w = (\Sigma N_i X_i^2)/(\Sigma N_i X_i)$. L_n and L_w were 1.08 μm and 1.78 μm, respectively (the reason those values are small will be examined in the Discussion). The ratio $\zeta = L_w/L_n$, which is a measure of the deviation of the distribution from the exponential ($\zeta = 2$ for exponential distribution) was 1.64. Manual and correlation method of determination of velocity gave 4.6 ± 0.6 μm/s and 5.2 ± 2.0 μm/s, respectively. With $D = 5$ μm the underestimation of velocity by the correlation method, due to the larger residence times of longer filaments, was 22%; after correction the mean velocity obtained by the correlation method becomes 6.3 ± 2.4 μm/s. The two were not different at 5% level of significance.

Comparison of number of moving filaments determined by correlation and manual methods

Correlation method can also be used to determine number of moving filaments. The rate of arrival of photons during one bin width, $\langle n \rangle$, must be equal to the rate of arrival of photons per rhodamine molecule per bin width, σ, multiplied by the number of rhodamine molecules in the area defined by the diaphragm. Let the average number of actin filaments in the area defined by the field diaphragm be $\langle N_c \rangle$. Then,

$$\langle n \rangle = \sigma \langle N_c \rangle. \quad (5)$$

The number of rhodamine molecules (not actin filaments!) contributing to the signal is $\langle N_c \rangle 400 L_n$, where L_n is the average length of actin filament, 400 is number of rhodamine molecules per 1 μm of actin filament (equal to the number of actin monomers/1 μm). Therefore,

$$\langle N_c \rangle = \langle n \rangle / 400 L_n \sigma. \quad (6)$$

Taking L_n = 1.08 μm (Fig. 9), $\langle n \rangle$ = 3,611 (average of 30 experiments), the average number of filaments in the field of view at a given time was $\langle N_c \rangle$ = 7.6 ± 4.5 (mean ± SD of 30 experiments) with SE = 0.82. This compares well with the average number of filaments within the diaphragm determined manually, $\langle N_m \rangle$: in 17 different fields of view there was 123 moving filaments in the area defined by a 10-μm diameter diaphragm, i.e., the average $\langle N_m \rangle$ was 7.24 ± 2.93 (mean ± SD of 17 determinations) with SE = 0.71. We can therefore state with 95% confidence that $\langle N_c \rangle$ and $\langle N_m \rangle$ were not different.

The average number of filaments contributing to the ACF measured in 204.8 s (assuming the filaments remained on the average for 2 s in the field of view) was 778 ± 463 (mean ± SD of 30 experiments).

The mean theoretical rms fluctuation β must be equal to the reciprocal of the average number of molecules observed by the photomultiplier (Elson and Magde, 1974):

$$\beta = 1/\langle N \rangle. \quad (7)$$

Theoretical value of β is therefore of the order of 13–14%. This is smaller than the experimental fluctuation of 34% in Fig. 6. Part of the different may be accounted for by the fact that $\langle N \rangle$ was overestimated. In correlation measurements some of the photons may have been contributed by stationary filaments and dust particles. In manual measurements, filaments which were moving outside the diaphragm might have been counted.

The value of the ACF at delay time 0, $G(0)$, is equal to the relative rms fluctuation β multiplied by the square of the mean photocurrent (Elson and Magde, 1974):

$$G(0) = \beta \langle i \rangle^2. \quad (8)$$

It follows from Eqs. 7 and 8 that $\langle N \rangle = \langle i \rangle^2 / G(0)$ and from Eqs. 5 and 7 that $\sigma = \langle n \rangle \beta$.

EXPERIMENTAL EXAMPLES

We applied the correlation method to study the dependence of velocity and the number of moving filaments in the in vitro assay on the ATPase activity of immobilized HMM. ATPase activity was affected by modification of HMM with two different SH group reagents, each of which affected different part of a hydrolytic cycle of HMM.

To carry out this experiment, we first verified that the velocity and the proportion of moving filaments did not depend on the position of observation of filament motion. We measured velocities at nine different positions on the cover slip, i.e., when the center of the objective was from 1 to 25 mm distant from the point where ATP was applied. There was no systematic variation of the velocity with position. The mean velocity in nine experiments was 6.9 μm/s (SD = 1.5, SE = 0.5 μm/s). The overall variation in velocity was small (SD/mean = 21%). Average number of moving filaments was calculated using Eq. 8. There was no systematic variation of the number of moving filaments with distance but the overall variation was large (SD/mean = 94%).

HMM modified with NEM

In the first series of experiments, we controlled ATPase activity of HMM by modificaton with NEM. Because velocity did not depend on the position of the objective, we investigated the influence of NEM modification on the velocity of actin filaments at random points across the slide (but typically at the center of the coverslip). We mixed intact HMM with increasing amounts of HMM which was 100% modified by NEM and measured the velocity and the number of moving filaments by the correlation and the manual methods. Because fully modified HMM had no K^+-EDTA ATPase activity, the loss of ATPase was proportional to the fraction of HMM modified with NEM. When the amount of NEM-modified fraction exceeded 0.5%, actin filaments became progressively broken into small fragments shorter than 0.5 μm. Fig. 10 shows the dependence of the velocity and the number of moving filaments on the loss of ATPase activity. All motion ceased when ATPase of HMM declined by only 2%. Similar result was reported by Warshaw et al. (1990).

In the Discussion we speculate that the movement is inhibited by fraction of HMMs which can not dissociate from actin even in the presence of ATP. Here we estimate this fraction by comparing the amount of NEM-HMM which sedimented in the ultracentrifuge together with F-actin in the absence and in the presence of ATP. Top panel of Fig. 11 shows SDS-PAGE patterns of acto-HMM before (lines 1 and 3) and the supernatant after (lines 2 and 4) ultracentrifugation in the absence (lines 1 and 2) and in the presence (lines 3 and 4) of ATP. Lines 1 and 2 show that when NEM-HMM-actin was sedimented in the absence of ATP, 9.5% of modi-

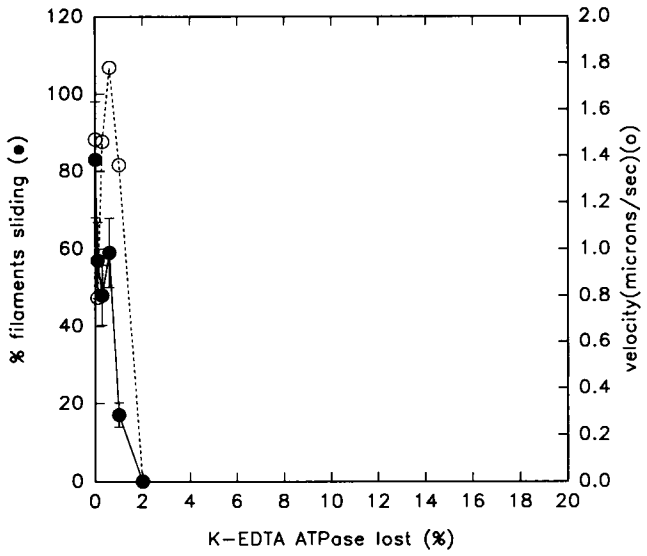

FIGURE 10 Velocity of filaments (*open circles*) and number of moving filaments (*filled circles*) as a function of degree of HMM modification with NEM.

fied HMM remained in the supernatant. This was denatured HMM which is unable to bind to actin. When the same complex was sedimented in the presence of ATP, the pattern shown in lines 3 and 4 was obtained. Fig. 11 (bottom panel) compares densitometric scans of lines 3 and 4. It shows that 25.8% of modified HMM remained in the supernatant after sedimentation in the presence of ATP. This included 9.5% of denatured HMM, HMM which has not been modified with NEM, and HMM which has been modified by NEM but was still sensitive to dissociation by ATP. We conclude that 74.2% of modified HMM is insensitive to ATP.

HMM modified with 5-IAF

We mixed intact HMM with increasing amounts of HMM which was 100% modified by 5-IAF and measured the velocity and the number of moving filaments by the correlation and the manual methods. Like in the case of NEM modification, the loss of ATPase was proportional to the fraction of HMM modified with 5-IAF. When the amount of 5-IAF-modified fraction exceeded 20%, actin filaments became progressively broken into small fragments shorter than 0.5 μm. The results are shown in Fig. 12. Velocity decreased hyperbolically with ATPase lost. The dependence was fitted to the equation $V = b(1 - I/I_0)/(a/I\ f_0 + I/I_0)$ where V is the velocity at the degree I of loss of K^+-EDTA ATPase, I_0 is the maximum ATPase lost and a and b are constants. The best least-squares non-linear fit, shown by solid line, gave $I_0 = 122$ units, $a = 17.20$, $b = 1.39$, $a/I_0 = 0.14$. The hyperbola was very curved: only 14% of ATPase loss was sufficient to decrease velocity to ½ of V_{max}. When 40% of heads were modified, V decreased by 80%. The significance of this finding is dealt with in the Discussion.

DISCUSSION

Correlation method

Fluorescence correlation spectroscopy has been used to determine kinetics of a chemical reaction (Magde et al., 1974; Elson and Magde, 1974), kinetics of multiple binding reactions (Icenogle and Elson, 1983), diffusion of solute (Magde et al., 1974) and flow (Magde and Elson, 1978, for review see Elson and Webb, 1975; Elson and Qian, 1989; Borejdo, 1980). The microscope was used in conjunction with the correlation method to study the two- and three-dimensional motion of a fluorescence marker (Koppel et al., 1976). In the present paper we combined the microscopical observation of individual molecules with the correlation method to measure velocities of filaments in in vitro motility assay. The number fluctuation method is well suited to measure actin velocity in motility assay because: (*a*) relative fluctuations are big ($\langle N \rangle$ is small); (*b*) rhodamine phalloidin is an ideal fluorophore for fluctuation experiments (it has a large absorption coefficient, high quantum yield when bound to actin and low quantum yield for photobleaching); (*c*) the mean "pathlength" of the motion of the filaments is larger than the typical diameter of the experimental area; (*d*) the mean velocity of many filaments can be measured in a short time, (*e*) the correlation method does not require imaging and thus does not suffer from the disadvantages associated with the video imaging of faint objects (e.g., lag, change of aspect ratio during playback from VCR).

The use of a laser beam for illumination is the main difference between our experimental arrangement (Fig. 1) and that which is usually employed to image individual actin filaments (e.g., Harada and Yanagida, 1988). Laser illumination is required in fluctuation experiments to eliminate problems associated with the instability of mercury lamp. At the same time we found laser illumination to be advantageous for the visualization of single actin filaments because the excitation beam has a more uniform profile and it is incident exactly at 45° to the plane of the dichroic mirror. Further, any photobleaching effects are smaller with monochromatic light.

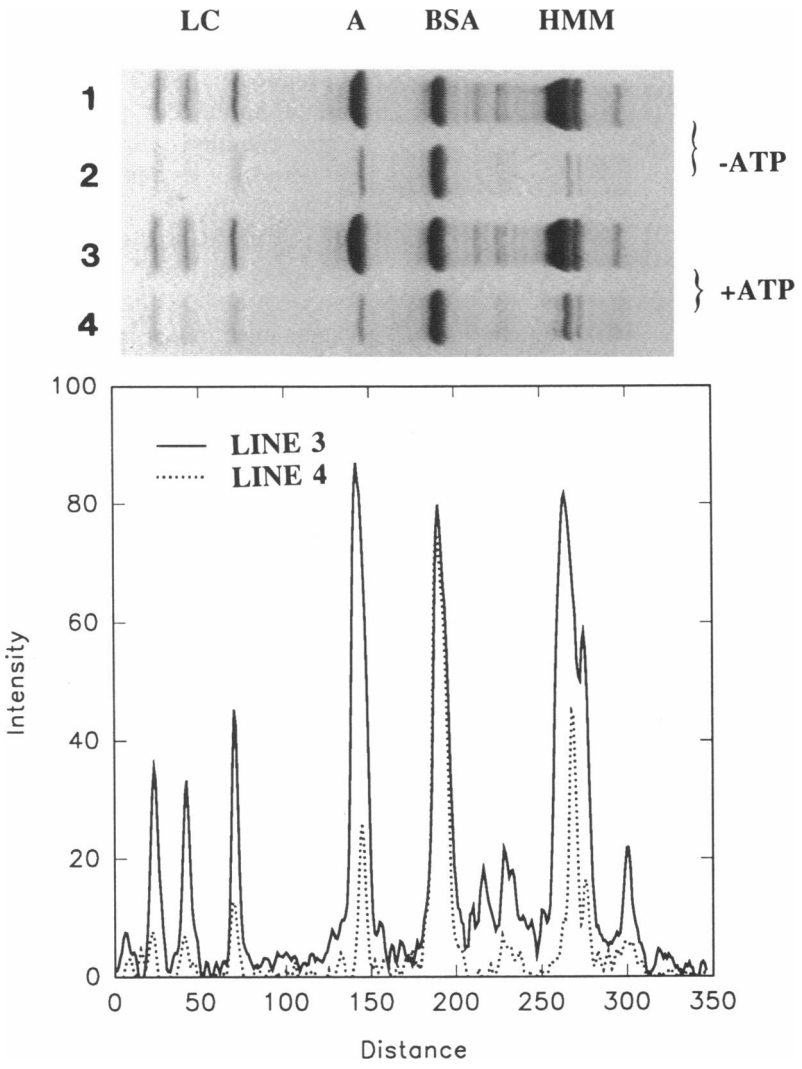

FIGURE 11 (*Top panel*) SDS-PAGE patterns of acto-HMM before and after ultracentrifugation in the absence and in the presence of ATP. Molar ratio NEM-HMM:actin 1:2, 1 mg/mL BSA. (*Line 1*) sample before ultracentrifugation. (*Line 2*) supernatant after ultracentrifugation in the absence of ATP at 40,000 rpm for ½ h at 4°C. (*Line 3*) sample containing 5 mM ATP before ultracentrifugation. (*Line 4*) supernatant after ultracentrifugation in the presence of 5 mM ATP. The major bands are: (from left to right) light chains 1, 2, and 3 (LC), actin (A), BSA (BSA), heavy chain of HMM (HMM) and myosin. (*Bottom*) densitometric scan of lines 3 and 4.

Differences with classical implementation

Effect of the diaphragm and of the distribution of filament lengths

Our experiments differ from classical number fluctuation measurements (Magde et al., 1974) in that: (*a*) we measured true two dimensional motion of macromolecules, whereas in earlier work two dimensionality was assured by the use of an auxiliary lens with a long focal length; (*b*) we used a field diaphragm to define sample volume (really a sample area); the laser intensity profile across the sample area was rectangular, not Gaussian; and (*c*) fluorescent objects were not infinitesimally small. Below we consider the effect of these differences.

As mentioned earlier, in a confocal microscope system such as used here, the decay time of the ACF of a three-dimensional diffusion of particles depends on the relative size of the diaphragm and the diameter of the laser beam. For example, when the diaphragm is smaller than the "beamwaist" of the laser, then the diffusion along the line of excitation becomes important and the shape of the ACF, as derived from two dimensional

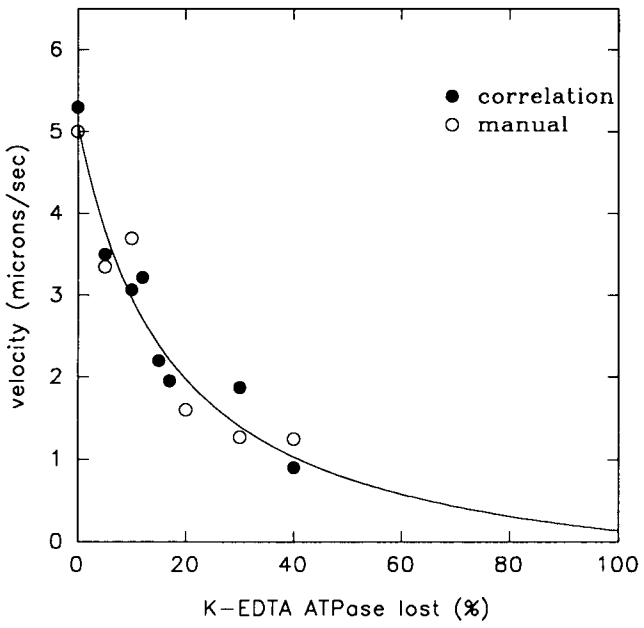

FIGURE 12 Velocity of filaments as a function of degree of HMM modification with 5-IAF. (*Filled circles*) velocity measured by correlation method, D = 10 μm. (*Open circles*) velocity measured manually. Solid line is the best least-squares nonlinear fit to the equation $V = b(1 - I/I_0)/(a/I_0 + I/I_0)$, where V is the velocity at the degree I of K^+-EDTA ATPase lost, I_0 is the maximum ATPase lost, and a and b are constants.

analysis, is no longer valid. Detailed analysis of the optics of the measurement system is required to obtain expression for the ACF (Qian and Elson, 1990). Instead of analyzing the system, we have carried out empirical calibration to show that in our system, in the case of three-dimensional diffusion of the assembly of uniform sized particles, the two-dimensional analysis of Elson and Magde (1974) was applicable. In the case of two-dimensional motion of particles with nonhomogeneous distribution of lengths, the Elson-Magde analysis was no longer valid, but we have found empirically that $\tau_D = \tau_{1/2}$ have good approximation.

The field diaphragm defines a sample area and not the volume. In classical implementation the laser beam itself defines the experimental volume. The intensity profile across this area is approximately rectangular, because the diaphragm selects the central portion of the defocussed Gaussian laser beam. The field diaphragm is necessary because the filaments move slowly. If it were not present, the filaments would translate the field of view in approximately 50 s, too long to carry out the measurements (for example, if τ_D were 10 s and $\delta\tau$ = 1 s, data collection would have to be 33 min to keep S/N at 10, see Eq. 2). The use of the field diaphragm has the effect of decreasing the effective aperture of the collection optics. In our arrangement the geometrical collection efficiency was 166 times smaller than in experiments of Magde et al (1974). Nevertheless, the rate of detection of fluorescent photons per molecule of the dye during one bin width (σ) was large because we used the dye with high extinction coefficient and quantum yield, and we observed slow motions. The size of the diaphragm (D) is critical for the proper design of the experiment: increasing the size of the diaphragm eliminates the complications arising from the fact that translating objects have finite size (see below). On the other hand increasing D decreases S/N, decreases the relative fluctuations and introduces complications arising from the pathlength of actin. In our experiments, unless otherwise stated, it was 5 μm.

Our experiments were complicated by the fact that the size of the fluorescent objects was non-negligible in comparison with the size of the diaphragm. For the spheres the error produced is small, because they all have uniform diameters. Indeed, in spite of the differences with classical implementation, Eq. 3 could be fitted to the experimental data well. Filaments, however, have a nonuniform distribution of lengths (Fig. 9) and this distribution changes with time after applying ATP. Thus, in rigor (Fig. 4*A*) filaments are long. After applying ATP filaments become shorter. This decrease is due to the fact that during movement, actin filament are acted upon by myosin heads for various times. One segment of a filament may be pushed by a head, while an adjoining segment may be at that moment held in rigor-like configuration by another head. The result is a shearing force, which breaks longer filaments. The same effect was reported by Toyoshima et al., 1990 and Uyeda et al., 1990. After ~9 min, when distribution shown in Fig. 9 was measured, the distribution reached a steady state and L_n decreased to 1.08 μm. This change in the distribution with time is most liley responsible for the fact that the ACF's are variable (Figs. 6*B*, and 7). We took measurements 8–10 min after adding ATP to the assay hoping that the filaments assumed equilibrium length, but this might not have been always the case. The nonuniform distribution of filament lengths is responsible for underestimation of velocity by the correlation method. Calculation shows that the underestimation due to the increased residency time in the illuminated area is of the order of D/L, where L is the length of a filament and D is the diameter of the aperture: filament with length L translates through an aperture of diameter D with speed V for $(D + L)/V$ s, while short filament translates for D/V s (thus long filaments remain in the field of view longer than short ones, even though both types move with the same velocity. The fractional increase in the time of translation is then $\phi = L/D$). In practice, fraction $\phi = L_n/D$ = 22% for D = 5 μm. The

underestimation due to the disproportional contribution to the correlation function by long filaments depends on the length distribution and has not been taken into account here.

Filaments often change the direction of motion. This movement also contributes to the fact that the correlation method underestimates the velocity, because the filaments remain in the field of view longer than if they moved only in straight lines. However, because the mean pathlength was comparable to the diameter of the diaphragm, the contribution of this effect was small.

To normalize for variability in ACF, we defined velocity as $D/\tau_{1/2}$. We observed good agreement between this velocity and the velocity determined manually. Thus, even though we did not attempt to derive an analytical solution for the ACF of filaments moving in two dimensions across the circular aperture, using $\tau_{1/2}$ as the characteristic time is justified. The accuracy of the method (SD/mean = 38%) is comparable to that of quasi-elastic light scattering (Fujime and Ishiwata, 1971). Even though the sample size is much greater for correlation measurements, the spread of velocities determined by the correlation method is larger than the spread determined manually (SD/mean = 13%). This is most likely due to a systematic change in filament length distribution during data collection. The absolute value of the velocity in our experiments was closer to the value reported by Spudich's group (Toyoshima et al., 1990; Uyeda et al., 1990) than Yanagida's group (Harada et al., 1990). However, because absolute velocity depends on many factors (e.g., temperature, number of inactive heads/active heads, length distribution of actin filaments) a direct comparison is not possible.

Varying the ATPase of HMM

NEM modification

The fact that velocity was found to be independent of the distance from the point of application of ATP was comforting, in view of the fact that in measuring the "step" distance the position of observation is not usually taken into account (Toyoshima et al., 1990; Uyeda et al., 1990; Harada et al., 1990). This finding allowed us to ignore the effect of position of observation in determining the dependence of the average velocity of filament motion on the ATPase activity.

All movement stopped when only 2% of EDTA-ATPase of NEM-modified was lost. NEM-HMM can no longer hydrolyze ATP but can bind strongly to actin (Pemrick and Weber, 1976). Such HMM can no longer be completely dissociated from actin by ATP. It makes sense to speculate that the effect of NEM modification was caused entirely by those cross-bridges which could not be dissociated from actin by ATP: these cross-bridges would provide large resistance to movement, and if their density per actin filament was large enough, they would stop all motion. To estimate this density we first correct for fraction of NEM-HMM which was still sensitive to dissociation by ATP. This fraction was 25.8% (Fig. 11) and the correction gives the fraction of heads at which all motion ceased as 1.5%. For every modified HMM there were thus, 67 active HMMs. It is not surprising therefore that actin filaments broke into small fragments. We assume here that those fragments were 0.5 μm long. Concentration of HMM was 0.6 mg/mL, i.e., the number of HMM molecules able to interact with 1 μm of actin filament was 1080 (band model, Uyeda et al., 1990). $1080 \times 1.5 \times 0.5/100 = 8$ NEM-modified HMM molecules per filament was therefore sufficient to stop the motion.

Our results re-emphasize the fact that quality of HMM is very important in evaluation of the "step distance" (the distance a filament is moved/ATP molecule split). This fact was recognized by Uyeda et al., 1990 and by Harada et al., 1990. When propelled by a mixture containing native and a few percent of inactive HMM, the distance would depend on the ability of ATP to dissociate the inactive fraction from actin. If inactive fraction were poorly dissociated from actin by ATP, the inactive fraction would provide large resistance to movement, and the distance would be small.

Varying the ATPase of HMM

5-IAF modification

The effect of modification of HMM with 5-IAF was very different than modification with NEM. This was due to the fact that each reagent modified different step in ATPase cycle. Interaction of 5-IAF-HMM with actin has not been kinetically characterized, but it is clear that ATP can completely dissociate 5-IAF-HMM from actin (Ando, 1984). It is not surprising, therefore, that adding progressively more modified HMM inhibited movement gradually. This inhibition could be fitted to Hill's hyperbola (but equally good fit was obtained to Eq. $V = a/(1 + bI)$). The velocity decrease with I was far from linear: our V-I curve had large curvature (small a/I_0). ATP turnover rate of S1 in solution, on the other hand, decreased linearly with I (Root et al., 1991), while in muscle fibers the dependence of velocity of contraction on inhibition of ATPase was neither linear nor hyperbolic: Crowder and Cooke (1984) have shown that when up to 60% of myosin heads in muscle fibers had SH_1 modified there was little effect on the contractile activity. Above 60% there was a decline in both force and velocity of shortening of modified fibers. The filament velocity in in vitro motility assay is thus different indication of mechanochemical activity than either the enzymatic velocity or the velocity of shortening of muscle fibers.

Our results point to the lack of simple correlation between the steady state ATPase activity and the in vitro motility. Similar lack of correlation has been seen before (Umemoto et al., 1989) and it was proposed (Umemoto and Sellers, 1990) that it is a demonstration of the fact that ATPase activity and motility are limited by different steps in the hydrolytic cycle.

We thank Dr. R. Takashi for modification of HMM and Professors M. F. Morales, E. L. Elson and D. Magde for valuable comments.

Supported by National Institutes of Health grant AR40095-01.

Received for publication 16 October 1991 and in final form 6 January 1992.

REFERENCES

Ando, T. 1984. Fluorescence of fluorescein attached to myosin SH_1 distinguishes the rigor state from the actin-myosin-nucleotide state. *Biochemistry* 23:375–381.

Borejdo, J., and M. F. Morales. 1977. Fluctuations in tension during contraction of single muscle fibers. *Biophys. J.* 20:315–334.

Borejdo, J., S. Putnam, and M. F. Morales. 1979. Fluctuations in polarized fluorescence: evidence that muscle cross-bridges rotate repetitively during contraction. *Proc. Natl. Acad. Sci. USA.* 76:6346–6350.

Borejdo, J. 1980. Application of fluctuation analysis to muscle contractility. *Curr. Top. Bioenerget.* 10:1–50.

Crowder, M. S., and R. Cooke. 1984. The effect of myosin sulphydryl modification on the mechanics of muscle contraction. *J. Muscle Res. Cell Motil.* 5:131–146.

Elson, E. L., and D. Magde. 1974. Fluorescence correlation spectroscopy. I. Conceptual basis and theory. *Biopolymers* 13:1–28.

Elson, E. L., and W. W. Webb. 1975. Concentration correlation spectroscopy. *Annu. Rev. Biophys. Bioeng.* 4:311–334.

Elson, E. L., and H. Qian. 1989. Interpretation of fluorescence correlation spectroscopy and photobleaching recovery in terms of molecular interactions. *Methods Cell Biol.* 30:307–332.

Englander, S. W., D. B. Calhoun, and J. J. Englander. 1987. Biochemistry without oxygen. *Anal. Biochem.* 161:300–306.

Fujime, S., and S. Ishiwata. 1971. Dynamic study of F-actin by quasielastic scattering of laser light. *J. Mol. Biol.* 62:251–265.

Harada, Y., and T. Yanagida. 1988. Direct observation of molecular motility by light microscopy. *Cell Motil.* 10:71–76.

Harada, Y., K. Sakudara, T. Aoki, D. D. Thomas, and T. Yanagida. 1990. Mechanochemical coupling in actomyosin energy transduction studied by in vitro movement assay. *J. Mol. Biol.* 216:49–68.

Houseal, T. W., C. Bustamante, R. F. Stump, and M. F. Maestre. 1989. Real-time imaging of single DNA molecules with fluorescence microscopy. *Biophys. J.* 56:507–516.

Huxley, H. E. 1990. Sliding filaments and molecular motile systems. *J. Biol. Chem.* 265:8347–8350.

Icenogle, R. D., and E. L. Elson. 1983. Fluorescence correlation spectroscopy and photobleaching recovery of multiple binding reactions. I. Theory and FCS measurements. *Biopolymers* 22:1919–1948.

Koppel, D. E. 1974. Statistical accuracy in fluorescence correlation spectroscopy. *Phys. Rev. A.* 10:1938–1945.

Koppel, D. E., D. Axelrod, J. Schlessinger, E. L. Elson, and W. W. Webb. 1976. Dynamics of fluorescence marker concentration as a probe of mobility. *Biophys. J.* 16:1315–1329.

Kron, S. J., and J. A. Spudich. 1986. Fluorescent actin filaments move on myosin fixed to a glass surface. *Proc. Natl. Acad. Sci. USA.* 83:6272–6276.

Kron, S. J., Y. Y. Toyoshima, T. Q. P. Uyeda, and J. A. Spudich. 1991. Assays for actin sliding movement over myosin coated surfaces. *Methods Enzymol.* 196:399–416.

Magde, D., E. L. Elson, and W. W. Webb. 1974. Fluorescence correlation spectroscopy. II. An experimental realization. *Biopolymers.* 13:29–61.

Magde, D., and E. L. Elson. 1978. Fluorescence correlation spectroscopy. III. Uniform translation and laminar flow. *Biopolymers.* 17:361–376.

Pemrick, S., and A. Weber. 1976. Mechanism of inhibition of relaxation ny *N*-ethylmaleimide treatment of myosin. *Biochemistry.* 15: 5193–5198.

Qian, H., and E. L. Elson. 1990. Characterization of confocal laser based microscope by digital image analysis: an optical sectioning microscopy approach. *In* Optical Microscopy for Biology. Wiley-Liss, New York. 119–130.

Qian, H., and E. L. Elson. 1991. Analysis of confocal laser-microscope optics for 3-D fluorescence correlation spectroscopy. *App. Optics.* 30:1185–1195.

Rabiner, L., and B. Gold. 1975 *In* Theory and Application of Digital Signal Processing. Prentice-Hall, Englewood, NJ. 367.

Root, D. D., P. Cheug, and E. Reisler. 1991. Catalytic cooperativity induced by SH_1 labeling of myosin filaments. *Biochemistry.* 30:286–294.

Sheetz, M. P., S. M. Block, and J. A. Spudich. 1986. Myosin movement in vitro: a quantitative assay using oriented actin cables from *Nitella. Methods Enzymol.* 134:531–544.

Spudich, J. A., and S. Watt. 1971. Regulation of rabbit muscle contraction. *J. Biol. Chem.* 246:4866–4871.

Tanford, C. 1963. *In* Physical Chemistry of Macromolecules. John Wiley and Sons, Inc., New York. 362.

Toyoshima, Y. Y., S. J. Kron, and J. A. Spudich. 1990. The myosin step size: measurement of the unit displacement per ATP hydrolyzed in an in vitro assay. *Proc. Natl. Acad. Sci. USA.* 87:7130–7134.

Umemoto, S., A. R. Bengur, and J. R. Sellers. 1989. Effect of multiple phosphorylations of smooth muscle and cytoplasmic myosins on movement in an in vitro motility assay. *J. Biol. Chem.* 264:1431–1436.

Umemoto, S., and J. R. Sellers. 1990. Characterization of in vitro motility assays using smooth muscle and cytoplasmic myosins. *J. Biol. Chem.* 265:14864–14869.

Uyeda, T. Q., S. J. Kron, and A. A. Spudich. 1990. Myosin step size. Estimation from slow sliding movement of actin over low densities of heavy meromyosin. *J. Mol. Biol.* 214:699–710.

Yanagida, T., T. Arata, and F. Oosawa. 1985. Sliding distance of actin filament induced by myosin cross-bridge during one ATP hydrolysis cycle. *Nature (Lond.).* 316:366–369.

Warshaw, D. M., J. M. Desrosiers, S. Work, and K. M. Trybus. 1990. Smooth muscle myosin cross-bridge interactions modulate actin filament sliding velocity in vitro. *J. Cell Biol.* 111:453–463.

Weeds, A. G., and B. Pope. 1977. Studies on the chymotryptic digestion of myosin. Effects of divalent cations on proteolytic susceptibility. *J. Mol. Biol.* 111:129–157.